

Thermo-hydraulic characteristics of laminar flow in a circular tube with porous metal cylinder inserts

Selvaraj.A.

M.TECH(Part-time) Thermal Engineering, Prist University, Vallam, Thanjavur

Abstract

Based on periodic surface models, a novel type of porous metal cylinder inserts (PMCI) was designed in this work to improve heat transfer. The thermo-hydraulic performance of laminar flow was numerically studied on a circular tube with PMCI. The effect of porosity, pore types, spacer length and clearance on the heat transfer performance was investigated. Liquid water was used as the working fluid. The numerical results show that the Nusselt number increases by 2.15-7.17 times the value of the plain tube, while the friction factor is augmented by 5.98-11.68 times. The performance evaluation criterion (PEC) value is 1.2-3.16. The computation results indicate that the Nusselt number and friction factor increase with the decrease in spacer length. Moreover, the effect of porosity on the thermo-hydraulic performance is also investigated. The results show that better PEC values of the tube can be obtained with smaller porosity. The effect of pore types on the heat transfer performance is also reported. Besides these findings, it indicates that the clearance is very sensitive to the heat transfer performance. The better heat transfer performance of the tube can be obtained with larger clearance. Compared with other inserts, the novel PMCI can transfer more heat than other inserts under the same pumping power which can guide us to optimize heat exchanges.

Keywords: Porous metal cylinder inserts; Periodic surface model; Heat transfer enhancement

1 Introduction

Heat exchangers have wide applications in various industrial fields such as refrigeration, chemical industry, air conditioning, and power generation, among others [1]. Considering the environmental problems and energy shortage, it is significant to enhance the heat transfer process in heat exchangers. Different theories and techniques have been reported for heat transfer enhancement. Generally, heat transfer enhancement techniques can be classified into two types: active techniques and passive techniques [2,3].

Due to the lack of requirement for external power, tube inserts are an effective method to enhance heat transfer in shell-and-tube heat exchangers, which are examples of passive techniques. Twisted-tape inserts [4-6] and modified tapes [7-13] have been widely used to improve heat transfer in both laminar and turbulent flow. Bas et al. [4] investigated the thermo-hydraulic characteristics in a tube with twisted-tape inserts experimentally. Multiple short-length twisted tapes resulted in pressure drops at least 50% lower than most full-length tapes [7]. Other kinds of inserts have also been developed, such as ring inserts [14-16], delta wing vortex generator [17] and small pipe inserts [18,19]. Kongkai paiboon et al. [15] experimentally found that the heat transfer coefficient could be increased by 137% in tubes with perforated conical-ring inserts. Tu et al. [18] developed a type of small pipe inserts that can guide fluid from the core area to the

boundary area through small pipes. Compared with other enhancement techniques, the inserts have the advantages of low cost, easy maintenance, and rapid installation, attracting substantial attention from researchers [19]. The mechanism of tube inserts is that swirl flow can be produced in the tube, which can enhance fluid mixing and disturb the boundary layer [20]. However, there is an increase in friction resistance accompanied by the enhancement of heat transfer. Therefore, the performance evaluation criterion (PEC) should be considered in developing heat transfer enhancement technology.

2 Physical model

The porous metal cylinder insert (PMCI) model will be constructed based on the periodic surface (PS) models introduced in Refs. [26,27]. Essentially, the PS model is an approximation of the triply periodic minimal surface, whose precise parametric form is difficult to determine [28]. Usually, the implicit PS can be written as [27,29]:

On the basis of PS models, this paper has developed a prototype system on the platform of Open CASCADE. The marching cube (MC) algorithm was introduced to accomplish the geometrical modeling of the PS. The details of the MC algorithm for PS modeling can be found in Ref. [28]. The porous metal cylinder inserts (PMCI), which can be easy to fabricate by selective laser melting (SLM), can be modeled based on the prototype system. One example of p-porous metal cylinder inserts (P-PMCI) with 50% porosity is designed in Fig. 1. From Fig. 2 another pore type of PMCI, named I-PMCI, is also modeled.

As shown in Fig. 3, the PMCI are suspended in the center of the plain tube. The inner diameter (D) of the plain tube is 14 mm, and the length (L) of a period of the tube ranges from 30 mm to 50 mm. The geometric parameters of PMCI are as follows: the PMCI length $l = 15$ mm; external diameter of PMCI $d = 8, 10, \text{ or } 12$ mm; thickness of PMCI $t = 1$ mm; the porosity of PMCI β

3 Numerical modeling

3.1 Governing equations

This paper adopted several assumptions during the numerical modeling, common to many researchers [30,31]. First, the flow is continuous, incompressible, Newtonian, isotropic and constant physical properties; second, the effect of gravity is negligible. Based on the above assumptions, the conservation equations, including continuity, momentum and energy equations, are as follows:

In Eq. (2), Eq. (3) and Eq. (4), ρ and p is fluid density and pressure; c_p and T are fluid specific heat and temperature; and λ and u are thermal conductivity and fluid viscosity, respectively.

3.2 Boundary conditions

To reduce the computation load, a period of the tube is selected as the computation region, as chosen by many researchers [30,31]. A periodic condition is specified at the inlet and outlet, and the upstream temperature is set to 293 K. No-slip conditions are imposed on the surfaces of the PMCI and the tube walls. Because increasing the velocity and velocity gradient in annular region and generating swirl flow are predominant in the heat transfer enhancement of inserts. The heat conduction within an insert and

the convection heat transfer between the porous inserts and the fluid are very limited and can be neglected [32]. Therefore, the porous cylinder inserts are also insulated during the numerical calculation in this paper. The constant heat flux condition is specified on the tube wall, and the value of the heat flux depends on the Reynolds number.

4 Validation of numerical method

4.1. Numeral solver model

A three-dimensional double-precision version of the CFD software is used to solve the above governing equations. All the equations with boundary conditions are discretized by the finite volume method. The ‘SIMPLE’ algorithm is adopted for pressure and velocity. The standard scheme is employed for the pressure term, while the momentum and energy terms are treated

using the second-order upwind scheme. The convergent criterion of 10^{-8} for energy is used, set as a relative residual of 10^{-6} for both continuity and momentum.

4.2. Mesh independence

The preprocessor of the CFD simulation is used for mesh generation. In order to validate the accuracy of numerical results, a mesh independence analysis was carefully conducted. Considering the similarity of mesh independence, this paper took the P-PMCI model as examples to conduct the mesh

independence analysis. The geometric parameters of the P-PMCI model are as follows: $D = 30\text{mm}$, $L = 30\text{ mm}$, $\beta = 34\%$, $d = 8\text{mm}$, $l = 15\text{ mm}$ and $t = 1\text{mm}$. Fig. 4 shows mesh in the cross section at $x = 20.7\text{mm}$ in the tube. Tetrahedral cells are used to mesh the tube and P-PMCI. To better simulate boundary layer effects, prism grids are extruded from the surface of the tube.

The region close to the outer and inner surface of P-PMCI is expected to be meshed with a high density of elements. To check the quality of the calculation, the mesh independence analysis was carefully investigated using three sets of grids (2 300 000, 3 200 000 and 4 100 000). The relative difference of the Nusselt number is within 4% between 3 200 000 and 4 100 000 cells models, and the relative difference of the friction factors is also within approximately 4%. Therefore, simulation results implies that the grid system of 3 200 000 is enough to capture the characteristics of the flow and used to perform the calculation

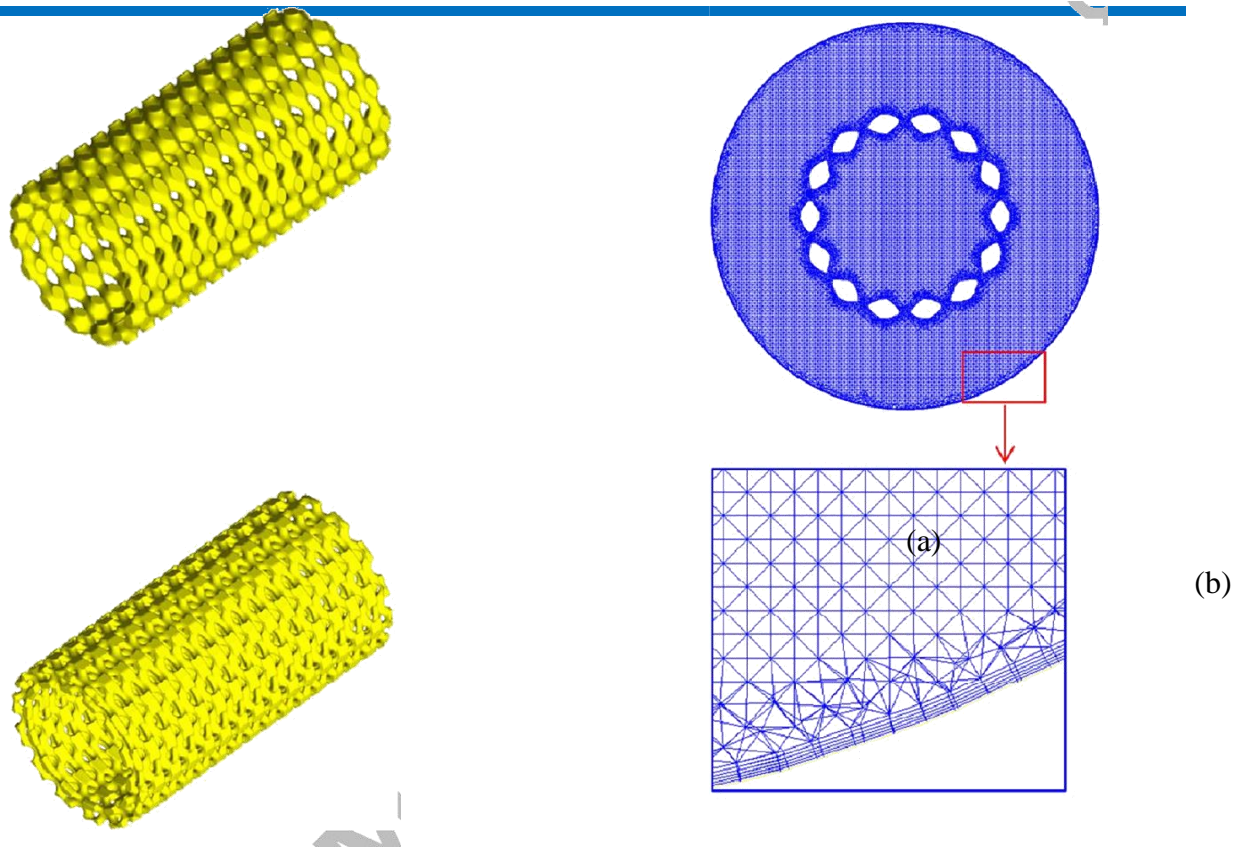


Fig. 1. Schematic of P-PMCI with 50% porosity: (a) 3D view of P-PMCI (b) Schematic of porous metal cylinder inserts

5 Results and discussion

5.1 The effect of porosity

Fig. 6a and b show the heat transfer performance of P-PMCI with different porosity at $D = 14\text{mm}$, $S/D = 2.14$, $\delta = 3\text{mm}$, and $d = 8\text{mm}$. Fig. 6b shows that Nusselt number ratio (Nu/Nu_p) increases with increasing Re number. Nusselt number ratio increase with decreasing porosity. The value of Nu for P-PMCI with 34% porosity (β) is better than for the rest, resulting in an enhancement of approximately 2.15-7.17 times the value for the plain tube in the Reynolds number range of 100-2050.

Friction factor decreased (Fig. 7a) while friction factor ratio (f/f_p) increased (Fig. 7b) with increasing Re number. In addition, the friction factor decreases with increasing porosity in Fig. 7a and b. Because the medium with higher porosity has good permeability [26], and fluid flow through the porous medium has less resistance. Therefore, the friction factor with higher porosity is smaller than that with low porosity.

Fig. 8 shows that the PEC values increase with increasing Reynolds number. In addition, the PEC values decrease with increasing porosity, but the effect on PEC is weak for the lower Reynolds

number. The *PEC* values for 34% porosity are approximately 1.19-3.16, which demonstrates that the P-PMCI has good overall thermo-hydraulic performance in the laminar flow regime. The empirical correlation of the Nusselt number and the friction factor of the tube fitted with P-PMCI with different porosity can be calculated

5.2 The effect of spacer length

Reynolds number for PMCI with different dimensionless spacer lengths ($S/D = 2.14$, $S/D = 2.86$, and $S/D = 3.57$) at $D = 14\text{mm}$, $\delta = 3\text{mm}$, $d = 8\text{mm}$ and $\beta = 34\%$. It shows that PMCI can enhance the heat transfer rate effectively in the laminar flow regime. Moreover, the Nusselt number rises with decreasing dimensionless spacer length. Data for PMCI with $S/D = 2.14$ are better than for others and result in an enhancement of approximately 2.15-7.17 times the value of the plain tube in the Reynolds number range of 100-2050. The data for $S/D = 2.865$ and $S/D = 3.57$ are enhanced by 1.93-5.92 and 1.78-5.16 times, respectively, for the ones in the plain tube.

The effect of the spacer length of the PMCI on the friction factor is depicted in Fig. 10a and b. The friction factor increases with decreasing spacer length. The data for $S/D = 2.14$ have the highest friction factor, with an increase of 5.98-11.68 times the value for the plain tube. The friction factor for inserts with $S/D = 2.86$ and $S/D = 3.57$ is increased 4.83-9.55 and 4.08-8.25 times, respectively.

The overall performance of the enhanced tube increases monotonically as the dimensionless spacer length decreases. The *PEC* values for $S/D = 2.14$ are approximately 1.19-3.16. The data for $S/D = 2.86$ lie in the range of 1.15-2.79. PMCI with $S/D = 3.57$ have *PEC*

values of 1.12-2.55, demonstrating that the PMCI has good thermo-hydraulic performance under laminar flow conditions. To obtain a better heat transfer rate, PMCI with a smaller spacer length should be adopted for applications with low Reynolds numbers. Therefore, a suitable spacer length must be taken into consideration in the design of the heat exchanger. The empirical correlation of the Nusselt number and the friction factor of the tube fitted with PMCI with different spacer lengths

6 Discussion

The numerical results indicated that the thermo-hydraulic characteristics are closely related to the structure of the PMCI. As shown in Fig. 3, the PMCI is suspended in the center of the plain tube, dividing the tube into an annular region and a core region. We take the velocity and temperature distribution as an example to study the effect of the geometric structure. The higher heat transfer rate is mainly attributed to the factors described below.

The contours of the velocity fields in the different cross sections of the enhanced tube are presented in Fig. 18 for the Reynolds number of 760. Section-a is in the front of the inlet of porous insert. Section-d is behind the outlet. Section-b and Section-c cross the PMCI. It can be drawn from Fig. 18 that the velocity of the annular region (Fig. 18b and c) is larger than that of section-a and section-d. Fig. 19 also shows that the larger velocity appears near wall in the annular region. In addition, Fig. 20 clearly shows that the peak velocity in the annular region for the enhanced tube is much higher than the velocities near the wall for plain tube, which helps to enhance the heat transfer. Therefore, higher heat transfer efficiency is contributed to the increase in the velocity and the velocity gradient in the annular region. And the insertion of PMCI greatly enhances the heat transfer performance.

The temperature contours of in the different cross sections of the enhanced tube are showed in Fig. 21, which is similar to the velocity contours. Fig. 21 and 22 clearly indicate that the temperature of tube wall in the annular region decreased, and the temperature gradient near wall becomes larger. In addition, the temperature distributions in the core region exhibit little difference between the enhanced tube and the plain tube in Fig. 23, but the temperature distribution in the annular region is very different. The wall temperatures are lower for the enhanced tube than for the plain tube, which can contribute to the heat transfer enhancement. As a result, the temperature gradient in the annular region increases, which results in higher heat transfer performance of tube. As mentioned above, higher heat transfer efficiency is mainly attributable to the following factors: the increase in the velocity and the velocity gradient in the annular region, and the horizontal and longitudinal vortexes generated on both sides of the inserts. These two factors work together to reduce the thickness of the thermal boundary layer and produce a high heat transfer rate. The effect of porosity on thermo-hydraulic characteristics can be explained as follows. As shown in Fig. 7a and b, the friction factor with higher porosity is low because the fluid flow through the medium with higher porosity has less resistance, allowing the fluid to flow through the porous media more easily. For the effect of the porosity on the heat transfer rate, the heat transfer is enhanced not only by the increased velocity and velocity gradient near the wall but also by the vortexes. However, the increase in the velocity has a great impact on the heat transfer rate. The porous medium with higher porosity has good permeability, so the velocity in the annular region is smaller for inserts with higher porosity. It is approximately 0.081 m/s for

inserts with 34% porosity and approximately 0.058 m/s for inserts with 70% porosity. Therefore, the thermal performance of inserts with lower

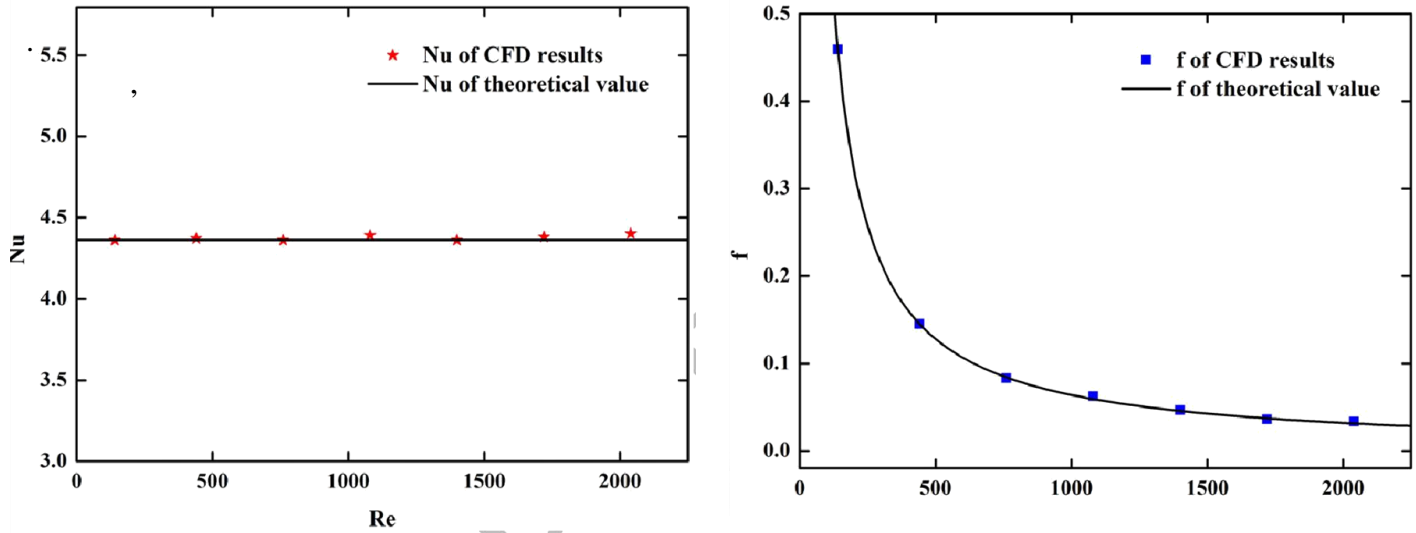


Fig. 5. Comparison between CFD results and theoretical values: (a) Nu , (b) f .

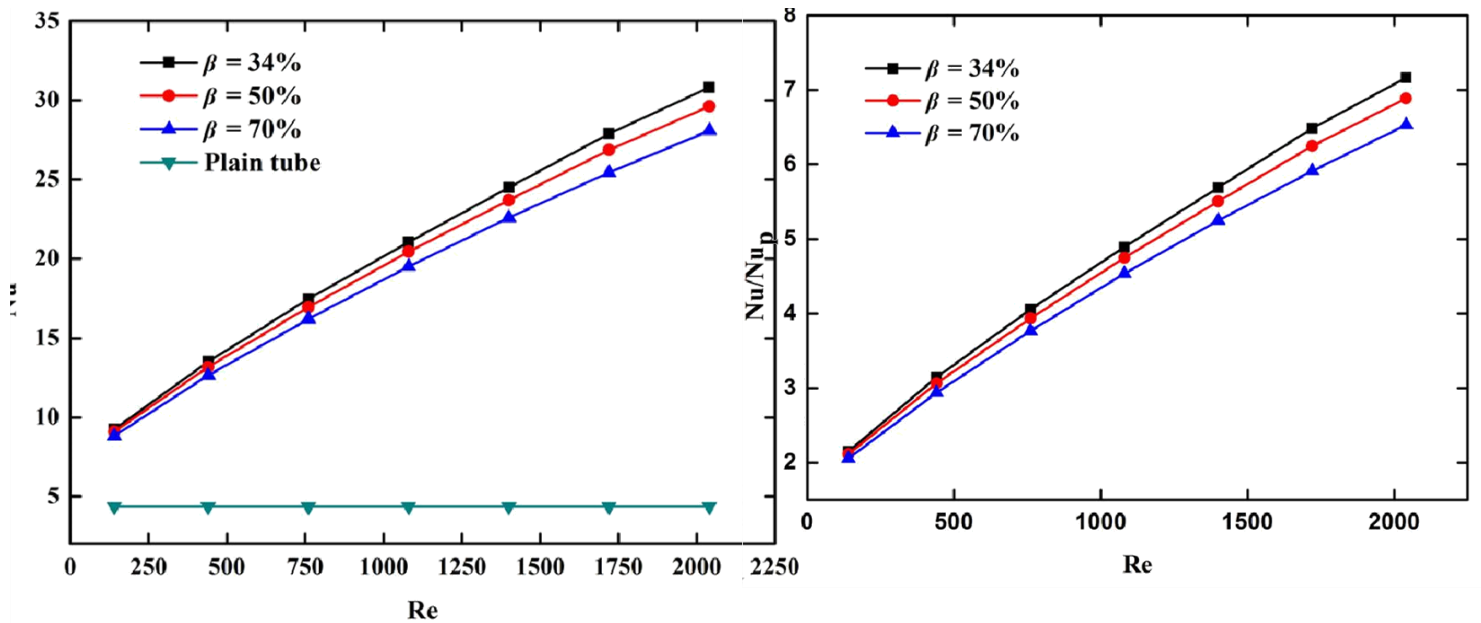


Fig. 6. Variation of Nu versus Re for inserts with different porosity: (a) Nu and (b) Nu/Nu_p

7 Conclusions

In this study, the thermo-hydraulic characteristics of porous metal cylinder inserts were analyzed in the laminar flow regime. The effects of spacer length, porosity, pore type and clearance on the heat transfer performance were studied by numerical simulations. The major conclusions can be summarized as follows:

(1) A novel type of porous metal cylinder inserts, with excellent heat transfer performance, is designed on the basis of periodic surface models.

(2) The heat transfer is enhanced not only by the larger velocity and velocity gradient in the annular region but also by the vortices along the inserts.

(3) The spacer length has a great effect on the heat transfer performance of PMCIs. The Nusselt number and friction factor both increase as the dimensionless spacer length decreases. To obtain a better heat transfer rate, PMCIs with a smaller spacer length should be employed. The heat transfer performance of PMCIs is affected by their porosity. The best heat transfer with PMCIs of 34% porosity is approximately 7.17 times the value for the plain tube. The friction factor increases with the decrease in porosity. The PEC values for 34% porosity are approximately 1.19-3.16. It is valuable to adopt a low porosity of PMCIs in the design of a heat exchanger.

(4) Heat transfer performance of PMCIs is affected by the pore types. Although the tube with the P-PMCI has better heat transfer performance, but the difference between P-PMCI and I-PMCI is limited. It is still meaningful to

select suitable porous structure for heat transfer enhancement.

The clearance is very sensitive to the heat transfer performance. Both Nusselt number and friction factor increase with an increase in clearance

References

[1] Liu S, Sakr M. A comprehensive review on passive heat transfer enhancements in pipe exchangers [J]. *Renewable and Sustainable Energy Reviews*, 2013, 19(1): 64–81.

[2] Cao Z, Xu J, Sun D, et al. Numerical simulation of modulated heat transfer tube in laminar flow regime [J]. *International Journal of Thermal Sciences*, 2014, 75(1): 171-183.

[3] Dewan A, Mahanta P, Raju K S, et al. Review of passive heat transfer augmentation techniques

[J]. *Proceedings of the Institution of Mechanical Engineers Part A Journal of Power and Energy*, 2004, 218(7): 509-527.

[4] Bas H, Ozceyhan V. Heat transfer enhancement in a tube with twisted tape inserts placed separately from the tube wall [J]. *Experimental Thermal and Fluid Science*, 2012, 41(41): 51-58.

[5] Vashistha C, Patil A K, Kumar M. Experimental investigation of heat transfer and pressure drop in a circular tube with multiple inserts [J]. *Applied Thermal Engineering*, 2015, 96: 117-129.



- [6] Eiamsa-Ard S, Kiatkittipong K. Heat transfer enhancement by multiple twisted tape inserts and TiO₂/water nanofluid [J]. *Applied Thermal Engineering*, 2014, 70(1): 896-924.
- [7] Ferroni P, Block R E, Todreas N E, et al. Experimental evaluation of pressure drop in round tubes provided with physically separated, multiple, short-length twisted tapes [J]. *Experimental Thermal and Fluid Science*, 2011, 35(7): 1357-1369.
- [8] Muthusamy C, Vivar M, Skryabin I, et al. Effect of conical cut-out turbulators with internal fins in a circular tube on heat transfer and friction factor [J]. *International Communications in Heat and Mass Transfer*, 2013, 44(44): 64-68.
- [9] Chang S W, Jan Y J, Jin S L. Turbulent heat transfer and pressure drop in tube fitted with serrated twisted tape [J]. *International Journal of Thermal Sciences*, 2007, 46(5): 506-518.
- [10] Chang S W, Yang T L, Jin S L. Heat transfer and pressure drop in tube with broken twisted tape insert [J]. *Experimental Thermal and Fluid Science*, 2007, 32(2): 489-501.
- [11] Murugesan P, Mayilsamy K, Suresh S, et al. Heat transfer and pressure drop characteristics in a circular tube fitted with and without V-cut twisted tape insert [J]. *International Communications in Heat and Mass Transfer*, 2011, 38(3): 329-334.
- [12] Promvonge P. Thermal Performance in square-duct heat exchanger with quadruple V-finned twisted tapes [J]. *Applied Thermal Engineering*, 2015, 91: 298-307.
- [13] Saysroy A, Eiamsa-Ard S. Periodically fully-developed heat and fluid flow behaviors in a turbulent tube flow with square-cut twisted tape inserts [J]. *Applied Thermal Engineering*, 2017, 112: 895-910.
- [14] Promvonge P, Eiamsa-Ard S. Heat transfer enhancement in a tube with combined conical-nozzle inserts and swirl generator [J]. *Energy Conversion and Management*, 2006, 47(18-19): 2867-2882.
- [15] Kongkaitpaiboon V, Nanan K, Eiamsa-Ard S. Experimental investigation of heat transfer and turbulent flow friction in a tube fitted with perforated conical-rings [M] *Experimental cinema* .: Studio Vista, 1971: 560-567.
- [16] Promvonge P. Heat transfer behaviors in round tube with conical ring inserts [J]. *Energy Conversion and Management*, 2008, 49(1): 8-15.